

1                                    **Genomic Locus Modulating IOP in the BXD RI Mouse Strains**

2  
3    Rebecca King<sup>1</sup>, Ying Li<sup>1</sup>, Jiaxing Wang<sup>1,2</sup>, Felix L. Struebing<sup>1</sup> and Eldon E. Geisert<sup>1</sup>

4  
5  
6    <sup>1</sup>Department of Ophthalmology, Emory University 1365B Clifton Road NE Atlanta GA,  
7    30322

8  
9    <sup>2</sup>Department of Ophthalmology, Tianjin Medical University General Hospital, Tianjin,  
10    China

11  
12  
13  
14  
15  
16    Corresponding Author:                    Eldon E. Geisert  
17    Professor of Ophthalmology  
18    Emory University  
19    1365B Clifton Road NE  
20    Atlanta GA 30322  
21    email: [egeiser@emory.edu](mailto:egeiser@emory.edu)  
22    Phone: 404-778-4239  
23  
24

25 **Abstract**

26

27 Purpose: Intraocular pressure (IOP) is the primary risk factor for developing glaucoma.  
28 The present study examines genomic contribution to the normal regulation of IOP in the  
29 mouse.

30

31 Methods: The BXD recombinant inbred (RI) strain set was used to identify genomic loci  
32 modulating IOP. We measured the IOP from 532 eyes from 34 different strains. The IOP  
33 data will be subjected to conventional quantitative trait analysis using simple and  
34 composite interval mapping along with epistatic interactions to define genomic loci  
35 modulating normal IOP.

36

37 Results: The analysis defined one significant quantitative trait locus (QTL) on Chr.8 (100  
38 to 106 Mb). The significant locus was further examined to define candidate genes that  
39 modulate normal IOP. There are only two good candidate genes within the 6 Mb over the  
40 peak, *Cdh8* (Cadherin 8) and *Cdh11* (Cadherin 11). Expression analysis on gene  
41 expression and immunohistochemistry indicate that *Cdh11* is the best candidate for  
42 modulating the normal levels of IOP.

43

44 Conclusions: We have examined the genomic regulation of IOP in the BXD RI strain set  
45 and found one significant QTL on Chr. 8. Within this QTL that are two potential  
46 candidates for modulating IOP with the most likely gene being *Cdh11*.

47

48

## 49 **Introduction**

50 Glaucoma is a diverse set of diseases with heterogeneous phenotypic presentations  
51 associated with different risk factors. Untreated, glaucoma leads to permanent damage of  
52 axons in the optic nerve and visual field loss. Millions of people worldwide are affected  
53 [1, 2] and it is the second leading cause of blindness in the United States [3]. Adult-onset  
54 glaucoma is a complex collection of diseases with multiple risk factors and genes with  
55 differing magnitudes of effects on the eventual loss of RGCs. The severity of the disease  
56 appears to be dependent on the interaction of multiple genes, age, and environmental  
57 factors [4]. There are also a number of phenotypic risk factors for POAG including: age,  
58 ethnicity, central corneal thickness and axial length[5]. The primary risk factor is an  
59 elevated intraocular pressure (IOP) [6]. There are known genetic mutations that affect  
60 IOP that result in inherited glaucoma [7, 8]. The prime example is MYOC, a protein  
61 secreted by the trabecular meshwork and mutations in this protein cause ER stress which  
62 results in a decrease in the function of the trabecular meshwork and an elevation in IOP  
63 [9, 10]. We know a considerable amount about the regulation of IOP from the production  
64 of aqueous humor to the outflow pathways. IOP is a complex trait affected by different  
65 tissues in the eye each of which is regulated by multiple genomic loci. Interestingly,  
66 there are very few studies that have identified genomic loci modulating normal IOP.

67

68 In the present study, we are using the BXD RI strain set that is particularly suited for the  
69 study of genetics and the effects on the severity of glaucoma. This genetic reference  
70 panel presently consists of 80 strains [11], and we are now in the unique position of being  
71 able to study the eyes of more than 80 strains with shuffled genomes from the two  
72 parental strains, C57BL/6J and the DBA/2J. There are over 7,000 break points in our  
73 current set of BXD strains. For this study, our group has measured IOP of 532 eyes from  
74 34 strains to identify genomic loci modulating IOP. A systems genetics approach to  
75 glaucoma is a relatively new branch of quantitative genetics that has the goal of  
76 understanding networks of interactions across multiple levels that link DNA variation to  
77 phenotype [12]. Systems genetics involves an analysis of sets of causal interactions  
78 among classic traits such as IOP, networks of gene variants, and developmental,  
79 environmental, and epigenetic factors. The main challenge is the need for comparatively

80 large sample size and the use of more advanced statistical and computational methods  
81 and models. We finally have a sufficiently large number of strains to use this approach  
82 [13, 14]. Our goal is now to combine data across several levels from DNA to ocular  
83 phenotype and analyze them with newly developed computational methods to understand  
84 pre-disease susceptibility to glaucoma along with the genetic networks modulating the  
85 response of the eye to elevated IOP.

86

87

## 88 **Methods**

89 Mice: This study measured the IOP in the 31 BXD strains of mice along with the parental  
90 strains the C57BL/6J mouse strain and the DBA/2J mouse strain. None of the BXD  
91 strains included in this study carried both mutations (*Tyrp1* and *Gpnmb*) known to cause  
92 the severe glaucoma phenotype observed in the DBA2/J strain. All of the mice in this  
93 study were between 60 and 120 days of age, a time before there is any significant  
94 elevation in IOP due pigment dispersion [15]. The data presented in this paper is based on  
95 measurements from 532 eyes with roughly equal numbers of male and female mice. All  
96 breeding stock was ordered from Jackson Laboratories (Bar Harbor, ME) and maintained  
97 at Emory. Mice were housed in the animal facility at Emory University, maintained on a  
98 12 hr light/dark cycle (lights on at 0700), and provided with food and water ad libitum.  
99 IOP measurement were made between 0900 and 1100. Both eyes were measured and the  
100 data from each eye was entered into the database. An induction–impact tonometer  
101 (Tonolab Colonial Medical Supply) was used to measure the IOP according to  
102 manufacturer’s instructions and as previously described (Saleh M, Nagaraju M, Porciatti  
103 2007; Nagaraju M, Saleh M, Porciatti V 2009). Mice were anesthetized with Avertin (334  
104 mg/kg) or ketamine/xylazine (100,15mg/kg). Three consecutive IOP readings for each eye  
105 were averaged. IOP readings obtained with Tonolab have been shown to be accurate and  
106 reproducible in various mouse strains, including DBA/2J (Wang et al., 2005). All  
107 measurements were taken approximately 10 minutes after the induction of anesthesia.  
108 These IOP measurements were made on mice prior to two different experimental  
109 procedures, blast injury to the eye or elevation of IOP by injection of magnetic beads into  
110 the anterior chamber. When we compared the IOP of animals anesthetized with Avertin

111 to those anesthetized with ketamine/xylazine over the entire dataset there was not  
112 significant difference between the two groups. We did a similar comparison looking only  
113 at the C57BL/6J mice with 11 mice anesthetized with Avertin (mean IOP 10.2, SD 0.15)  
114 and 27 mice anesthetized with ketamine/xylazine (mean IOP 11.2, SD 2.9) and there was  
115 no statistically significant difference between the two groups using a student *t*-test.

116

117 **Interval Mapping of IOP Phenotype:** The IOP data will be subjected to conventional  
118 QTL analysis using simple and composite interval mapping along with epistatic  
119 interactions. Genotype was regressed against each trait using the Haley-Knott equations  
120 implemented in the WebQTL module of GeneNetwork [16] [17] [18]. Empirical  
121 significance thresholds of linkage are determined by permutations [19]. We correlate  
122 phenotypes with expression data for whole eye and retina generated [13, 20, 21].

123

124 **Immunohistochemistry:** For immunohistochemical experiments mice were deeply  
125 anesthetized with a mixture of 15 mg/kg of xylazine (AnaSed) and 100 mg/kg of  
126 ketamine (Ketaset)

127 and perfused through the heart with saline followed by 4% paraformaldehyde in  
128 phosphate buffer (pH 7.3). The eye were embedded in paraffin as described by Sun et al.,  
129 [22]. The eyes were dehydrated in a series of ethanol and xylenes changes for 20 minutes  
130 each (50% ETOH, 70% ETOH, 90% ETOH, 95% ETOH, two changes of 100% ETOH,  
131 50% ETOH with 50% xylenes, two changes of 100 xylenes, two changes of paraffin. The  
132 eyes were then embedded in paraffin blocks. The eye were sectioned with a rotary  
133 microtome at 10 $\mu$ m and mounted on glass slides. The sections were deparaffinized and  
134 rehydrated. The sections were rinsed in PBS, and then placed in blocking buffer  
135 containing 2% donkey serum, 0.05% DMSO and 0.05% Triton X-100 for 30 min. The  
136 sections were rinsed in PBS, and then placed in blocking buffer containing 2% donkey  
137 serum, 0.05% DMSO and 0.05% Triton X-100 for 30 min. The sections were incubated  
138 in primary antibodies (1:500) against Cadherin 11 (Thermofisher, Cat. #71-7600,  
139 Waltham, MA) overnight at 4°C. After rinsing, the sections were incubated with  
140 secondary antibody conjugated to AlexaFluor-488 (donkey anti-rabbit, Jackson  
141 Immunoresearch Cat #711-545-152, Westgrove, PA) , (1:1000), for 2 hours at room

142 temperature. The sections were then rinsed 3 times in PBS for 15 minutes each. Then  
143 they were counterstained with TO-PRO-3 iodide was purchased from Invitrogen (T3605,  
144 Invitrogen, Eugene OR). The slides were flooded with Fluoromount-G (SouthernBiotech  
145 Cat #. 0100-01, Birmingham, AL), and covered with a coverslip. All images were  
146 photographed using on Nikon Eclipse TE2000-E (Melville, NY) confocal and images  
147 were acquired by Nikon's EZ-C1 Software (Bronze Version, 3.91).

148

149 **PCR Validation:** Reverse transcription-quantitative polymerase chain reaction (RT-  
150 qPCR) were used to validate the mRNA expression level of Cdh11 and Cdh8 and Myoc  
151 in whole eyes of C57BL/6J mice. Primers were designed for Cdh11, Cdh8 and Myoc  
152 using Primer BLAST-NCBI so that predicted PCR products were approximately 150bp.  
153 The cycle threshold values were normalized to a mouse housekeeping gene  
154 peptidylprolyl isomerase A (Ppia). Sequences of the PCR primers are listed in  
155 supplementary Table I. PCR reactions were carried out in 10 $\mu$ l reactions containing 5 $\mu$ l  
156 of 2x QuantiTect SYBR Green PCR Master Mix (Qiagen, Cat #204141 Hilden,  
157 Germany), 0.5  $\mu$ l of forward primer (0.5 $\mu$ M), 0.5  $\mu$ l of reverse primer (0.5  $\mu$ M), 2 $\mu$ l of  
158 template cDNA(10ng) and 2 $\mu$ l of RNA free H<sub>2</sub>O. PCR of mouse genes was performed  
159 using a program beginning at 95°C for 15 min, followed by 40 cycles of reaction with  
160 denaturation at 94°C for 15 sec, annealing at 59°C for 30 sec and extension at 72°C for  
161 30 sec of each cycle.

162

163

## 164 **Results**

165 The overall goal of the present investigation was to determine if specific genomic loci  
166 modulate IOP in the BXD RI strains. IOP was measured in 532 eyes form 31 BXD RI  
167 strains and the two parental strains C57BL/6J mouse and DBA2/J mouse. To create a  
168 mapping file the strain averages and standard errors were calculated (Figure 1). The IOP  
169 measured across the 33 strains was 13.2 mmHg and the standard deviation was 1.5  
170 mmHg. The strain with the lowest IOP was DBA2/J, with an average IOP of 10.9 mmHg.  
171 The strain with the highest IOP was BXD48 with an average IOP of 17.1 mmHg. The  
172 IOP of the parental strains was 11.6 mmHg for the C57BL/6J and 10.9 mmHg for the

173 DBA2/J. This is a substantial amount of genetic transgression across the BXD RI strain  
174 set. This type of phenotypic variability is a clear indication that IOP is in fact a complex  
175 trait. These data can also be used to calculate the heritability of IOP. Figure 1 reveals a  
176 considerable variability in the IOP from strain to strain and the standard error for each  
177 strain is rather small. This type of data suggests that the genetic variability has a greater  
178 effect than the environmental variability. These data can be used to calculate the  
179 heritability of IOP. To calculate heritability ( $H^2$ ) is the genetic variance ( $V_g$ ) of the trait is  
180 divided by the sum of genetic variance plus the environmental variance ( $V_g + V_e$ ). The  
181 genetic variance can be estimated by taking the standard deviation of the mean of IOP for  
182 each strain ( $V_g = 1.5$  mmHg). The environmental variance can be estimated by taking the  
183 mean of the standard deviation across the strain ( $V_e = 3.3$  mmHg). Using the formula for  
184 heritability,  $H^2 = V_g / (V_g + V_e)$ , the calculation of  $1.5 \text{ mmHg} / (1.5 \text{ mmHg} + 3.3 \text{ mmHg})$   
185 reveals that  $H^2 = 0.316$ . Thus, IOP is a heritability trait in the BXD RI strain set.

186

187 **Genome Wide Mapping:** Taking the average IOP from 33 strains of mice we performed  
188 an unbiased genome wide scan to identify genomic loci (QTLs) that modulate IOP. The  
189 genome-wide interval map (Figure 2) identifies on significant peak on Chr. 8. Examining  
190 an expanded view of Chr.8, 90 to 120 Mb (Figure 3), the peak of the IOP QTL reaches  
191 significance from 100 Mb to 106 Mb. BXD strains with higher IOPs (Figure 3B) tend to  
192 have the C57BL/6J allele (red) and strains with lower IOPs tend to have the DBA2/J  
193 allele (green). When the distribution of genes within this region is examined (gene track  
194 Figure 3A) the significant portion of the QTL peak covers a region of the genome that is  
195 a gene desert. Within this region there are only 5 genes: *Arl5a* (ADP-ribosylation factor-  
196 like 5a), *Cdh11* (cadherin11), *Cdh8* (cadherin 8), *Gm15679* (predicted gene 15679) and  
197 *Rplp0* (ribosomal protein, large, P0). Using the tools available on GeneNetwork  
198 ([genenetwork.org](http://genenetwork.org)) we are able to identify potential candidates for modulating IOP in the  
199 BXD RI strains. The candidate genes can either be genomic elements with cis-QTLs or  
200 they can be genes with nonsynonymous SNPs changing protein sequence. Within this  
201 region there are only two putative candidate genes. There are cisQTL for *Cdh11* (exon  
202 probes 17512155 and 17512156, build 2016-12-12 GeneNetwork). There are two genes  
203 in this region with non-synonymous SNPs, *Cdh11* and *Cdh8*. Thus, there is a single QTL

204 modulating IOP and this peak lies in a gene desert with only two good candidate genes  
205 *Cdh11* and *Cdh8*.

206

207 For the initial evaluation of the two candidate genes we examined their expression level  
208 in microarray datasets hosted on GeneNetwork: the eye database (Eye M430v2 (Sep08)  
209 RMA) and retina database (DoD Retina Normal Affy MoGene 2.0 ST (May15) RMA  
210 Gene Level). In the eye dataset, the highest level of expression for a *Cdh11* probe set  
211 (1450757\_at) is 10.8 Log<sub>2</sub>, while for *Cdh8* (1422052\_at) the highest level of expression  
212 is 7.3 Log<sub>2</sub>. For this dataset the mean expression of mRNA in the retina is set to 8. Thus,  
213 *Cdh11* is expressed at levels higher than the mean and *Cdh8* is expressed at levels below  
214 the average expression level. Furthermore, in the whole eye database, there is over an 8-  
215 fold increase in expression of *Cdh11* relative to *Cdh8*. In the retina database, *Cdh11*  
216 (probe set 17512153) had an expression level of 10.9 and *Cdh8* (probe set 17512121) had  
217 an expression level of 9.3, indicating that within the retina proper *Cdh11* expression is  
218 2-fold higher than *Cdh8*.

219

220 To confirm the expression levels of *Cdh11* and *Cdh8* in the eye, we examined the levels  
221 of mRNA in the whole eye by RT-qPCR. In 4 biological replicate RNA samples, we  
222 examined the levels of *Cdh11*, *Cdh8* and *Myoc* (a marker of trabecular meshwork cells,  
223 [23]). Our PCR analysis confirmed the general findings of the microarray data sets. In  
224 the 4 biological samples of whole eye, *Cdh11* was more highly expressed than *Cdh8*. The  
225 average of the 4 samples demonstrated a more than 2-fold higher expression of *Cdh11*  
226 than *Cdh8*. *Myoc* was also expressed at a higher level than *Cdh8* but at approximately at  
227 the same level as *Cdh11*. All of these data taken together indicate that *Cdh11* is the prime  
228 candidate for an upstream modulator of IOP.

229

230 **Distribution of Cadherin 11 in the Eye:** To determine if cadherin 11 is found in  
231 structures associated with the control of IOP, we stained sections of the eye for cadherin  
232 11. In these sections, there was a considerable amount of antibody-specific staining (Fig.  
233 4A). This label is not observed in control sections stained with secondary antibody only  
234 (Fig. 4B). There is extensive labeling of all layers of the cornea. The epithelium of the



235 ciliary body is also heavily labeled as well as labeling of pars plana. There is also light  
236 labeling of the retina. At higher magnification (Fig. 4C), clear labeling of the trabecular  
237 meshwork (arrow). Thus, cadherin 11 is expressed in the cells of the trabecular  
238 meshwork, the primary structure involved in regulating IOP.

239

240

## 241 **Discussion**

242 The normal regulation of intraocular pressure is a balance between production in the  
243 ciliary body and outflow [24, 25]. In the human, IOP ranges can range from a relatively  
244 low pressures to extremely high that occur in acute angle closure glaucoma. It is  
245 generally accepted that the “normal” range for IOP in humans is from 12mmHg to  
246 22mmHg [26, 27]. In addition, monitoring throughout the day reveals IOP is pulsatory  
247 and has a diurnal variability [28]. These findings tell an interesting story about the  
248 regulation of pressure in the eye; however, the primary driving force behind the intense  
249 investigation of IOP in humans is that fact that it is the primary risk factor for developing  
250 glaucoma [29]. Furthermore, all of the current treatments for glaucoma center around  
251 lowering IOP either by pharmacological approaches or surgery [30, 31].

252

253 The association of elevated IOP and glaucoma, has driven most of the study of IOP in  
254 human populations [5, 32, 33]. Most of these studies involve the study of glaucoma, but  
255 a few have a primary focus on the regulation of IOP. These studies have found that  
256 IOP is a heritable trait with estimates of heritability ranging from 0.39 to 0.64 [6, 34-36].  
257 In the present study, we found that the heritability of IOP in the BXD RI strains was 0.36.  
258 Thus, the mouse strains demonstrated a heritability near the lower end of the human  
259 populations. The interest has prompted studies to identify genes regulating IOP. In a  
260 genome-wide association study of IOP involving 11,972 subjects, significant associations  
261 were observed with SNPs in two genes, *GAS7* and *TMCO1* [37]. Both of these genes are  
262 expressed at high levels in the ciliary body and trabecular meshwork [38] and both of the  
263 genes interact with known glaucoma risk genes [37]. *TMCO1* is also known to be  
264 associated with severe glaucoma risk [39].

265

266 In an effort to understand the regulation of IOP and its effects on the retina, many  
267 research groups have used inbred mouse strains [40-44]. IOP varies widely across  
268 different strains of mice [40, 45], ranging from a low of 11mmHg in the BALB/c mouse  
269 strain to a high of 19mmHg in the CBA/Ca mouse strain. In the present study, the  
270 average measured IOP across the 34 strains was 13.2mmHg. The lowest measured IOP  
271 was 10.9mmHg in the DBA/2J strain and the highest was 17.1mmHg in the BXD48  
272 strain. Using the variability across the BXD RI strains we were able to map a single  
273 significant QTL on Chr. 8 in the mouse. The peak of the QTL was in a gene desert and  
274 within this region there were only two potential candidate genes that could be modulating  
275 IOP in the BXD strain set. Based on expression of mRNA in the eye microarray dataset  
276 and the findings of real time PCR *Cdh11* appears to be the best candidate. *Cdh11* is  
277 expressed approximately 8-fold higher in the eye than is *Cdh8*. Furthermore, previous  
278 study [46] found *CDH11* to be highly expressed in cultured human trabecular meshwork  
279 cells. We found that Cadherin 11 is expressed in the trabecular meshwork using indirect  
280 immunohistochemistry. All of these data suggest that the expression Cadherin 11 in the  
281 trabecular meshwork modulates IOP across the BXD RI strain set.

282

283 How is it possible that a cadherin can modulate IOP in the mouse eye? IOP is regulated  
284 by fluid resistance at the trabecular meshwork and Schlemm's canal [47, 48]. The  
285 stiffness of these structures is determined by the extracellular matrix within the trabecular  
286 meshwork and Schlemm's canal and the contractile nature of the cells themselves (Zhou  
287 et al. 2012) inner wall was considered to be the most important player regulating such  
288 resistance [49-51]. The dysregulation or poor organization of extracellular matrix may  
289 increase the fluid resistance, leading to an elevation of the IOP. *Cdh11* was recently  
290 revealed to be a novel regulator of extracellular matrix synthesis and tissue  
291 mechanics[52] , and it is also found to be highly expressed in cultured human trabecular  
292 meshwork cells [46]. It is possible that the IOP can be regulated by *Cdh11* and related  
293 pathways by altering the extracellular matrix structure of the trabecular meshwork. Future  
294 studies about the role of *Cdh11* in the trabecular meshwork may give insights into the  
295 mechanism of IOP modulation.

296

297

298

299

300 Acknowledgements: We would like to thank the Robert W William and his group for  
301 providing a wealth of bioinformatic resources on GeneNetwork.org. We thank Chelsey  
302 Faircloth for her assistance in immunostaining. This study was supported by an  
303 Unrestricted Grand from Research to Prevent Blindness, NEI grant R01EY178841  
304 (E.E.G.), Owens Family Glaucoma Research Fund, P30EY06360 (Emory Vision Core)  
305 and DoD CDMRP Grant W81XWH1210-1-255 from the USA Army Medical Research  
306 & Materiel Command and the Telemedicine and Advanced Technology (E.E.G.).

307

308

309

310 **References**

311

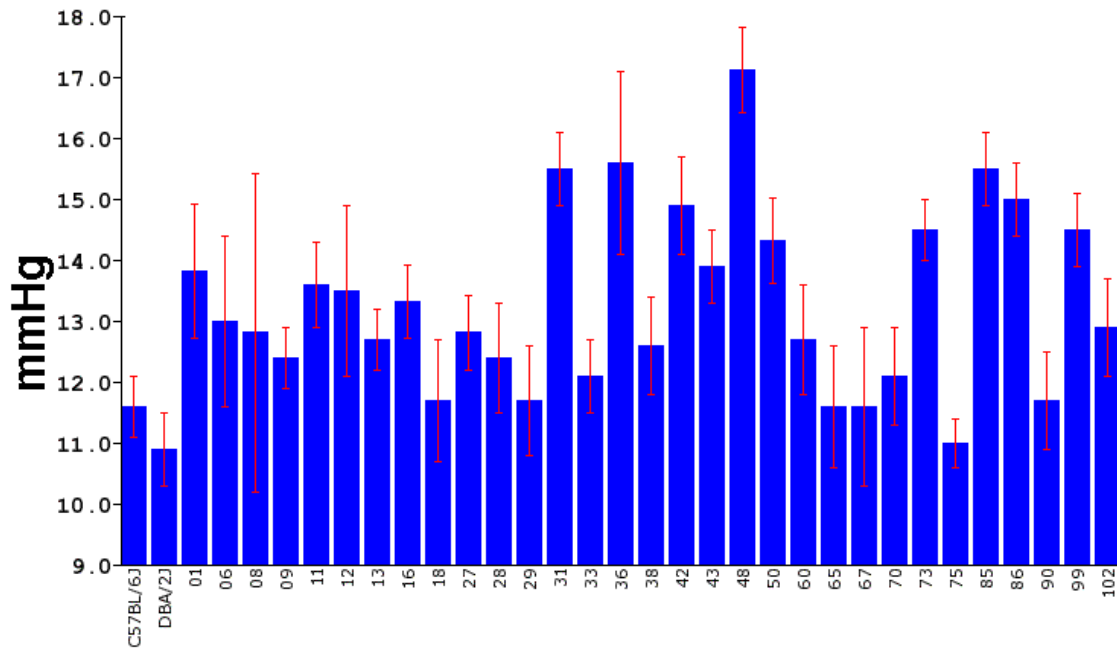
- 312 1. European Glaucoma Prevention Study G, Miglior S, Pfeiffer N, Torri V,  
313 Zeyen T, Cunha-Vaz J, Adamsons I. Predictive factors for open-angle glaucoma  
314 among patients with ocular hypertension in the European Glaucoma Prevention  
315 Study. *Ophthalmology* 2007; 114(1):3-9.
- 316 2. Leske MC, Heijl A, Hyman L, Bengtsson B, Dong L, Yang Z, Group E.  
317 Predictors of long-term progression in the early manifest glaucoma trial.  
318 *Ophthalmology* 2007; 114(11):1965-72.
- 319 3. Medeiros FA, Sample PA, Zangwill LM, Bowd C, Aihara M, Weinreb RN.  
320 Corneal thickness as a risk factor for visual field loss in patients with  
321 preperimetric glaucomatous optic neuropathy. *Am J Ophthalmol* 2003;  
322 136(5):805-13.
- 323 4. Herndon LW, Weizer JS, Stinnett SS. Central corneal thickness as a risk  
324 factor for advanced glaucoma damage. *Arch Ophthalmol* 2004; 122(1):17-21.
- 325 5. Gordon MO, Beiser JA, Brandt JD, Heuer DK, Higginbotham EJ, Johnson  
326 CA, Keltner JL, Miller JP, Parrish RK, 2nd, Wilson MR, Kass MA. The Ocular  
327 Hypertension Treatment Study: baseline factors that predict the onset of primary  
328 open-angle glaucoma. *Arch Ophthalmol* 2002; 120(6):714-20; discussion 829-30.
- 329 6. Klein BE, Klein R, Lee KE. Heritability of risk factors for primary open-  
330 angle glaucoma: the Beaver Dam Eye Study. *Invest Ophthalmol Vis Sci* 2004;  
331 45(1):59-62.
- 332 7. Stone EM, Fingert JH, Alward WL, Nguyen TD, Polansky JR, Sunden SL,  
333 Nishimura D, Clark AF, Nystuen A, Nichols BE, Mackey DA, Ritch R, Kalenak  
334 JW, Craven ER, Sheffield VC. Identification of a gene that causes primary open  
335 angle glaucoma. *Science* 1997; 275(5300):668-70.
- 336 8. Wiggs JL. Genetic etiologies of glaucoma. *Arch Ophthalmol* 2007;  
337 125(1):30-7.
- 338 9. Joe MK, Sohn S, Hur W, Moon Y, Choi YR, Kee C. Accumulation of  
339 mutant myocilins in ER leads to ER stress and potential cytotoxicity in human  
340 trabecular meshwork cells. *Biochem Biophys Res Commun* 2003; 312(3):592-  
341 600.
- 342 10. Kasetti RB, Phan TN, Millar JC, Zode GS. Expression of Mutant Myocilin  
343 Induces Abnormal Intracellular Accumulation of Selected Extracellular Matrix  
344 Proteins in the Trabecular Meshwork. *Invest Ophthalmol Vis Sci* 2016;  
345 57(14):6058-69.
- 346 11. Peirce JL, Lu L, Gu J, Silver LM, Williams RW. A new set of BXD  
347 recombinant inbred lines from advanced intercross populations in mice. *BMC*  
348 *Genet* 2004; 5:7.
- 349 12. Mozhui K, Ciobanu DC, Schikorski T, Wang X, Lu L, Williams RW.  
350 Dissection of a QTL hotspot on mouse distal chromosome 1 that modulates  
351 neurobehavioral phenotypes and gene expression. *PLoS Genet* 2008;  
352 4(11):e1000260.

- 353 13. Geisert EE, Lu L, Freeman-Anderson NE, Templeton JP, Nassr M, Wang  
354 X, Gu W, Jiao Y, Williams RW. Gene expression in the mouse eye: an online  
355 resource for genetics using 103 strains of mice. *Mol Vis* 2009; 15:1730-63.
- 356 14. Freeman NE, Templeton JP, Orr WE, Lu L, Williams RW, Geisert EE.  
357 Genetic networks in the mouse retina: growth associated protein 43 and  
358 phosphatase tensin homolog network. *Mol Vis* 2011; 17:1355-72.
- 359 15. Anderson MG, Smith RS, Hawes NL, Zabaleta A, Chang B, Wiggs JL,  
360 John SW. Mutations in genes encoding melanosomal proteins cause pigmentary  
361 glaucoma in DBA/2J mice. *Nat Genet* 2002; 30(1):81-5.
- 362 16. Chesler EJ, Lu L, Shou S, Qu Y, Gu J, Wang J, Hsu HC, Mountz JD,  
363 Baldwin NE, Langston MA, Threadgill DW, Manly KF, Williams RW. Complex trait  
364 analysis of gene expression uncovers polygenic and pleiotropic networks that  
365 modulate nervous system function. *Nat Genet* 2005; 37(3):233-42.
- 366 17. Rosen GD, La Porte NT, Diechtiareff B, Pung CJ, Nissanov J, Gustafson  
367 C, Bertrand L, Gefen S, Fan Y, Tretiak OJ, Manly KF, Park MR, Williams AG,  
368 Connolly MT, Capra JA, Williams RW. Informatics center for mouse genomics:  
369 the dissection of complex traits of the nervous system. *Neuroinformatics* 2003;  
370 1(4):327-42.
- 371 18. Carlborg O, De Koning DJ, Manly KF, Chesler E, Williams RW, Haley CS.  
372 Methodological aspects of the genetic dissection of gene expression.  
373 *Bioinformatics* 2005; 21(10):2383-93.
- 374 19. Churchill GA, Doerge RW. Empirical threshold values for quantitative trait  
375 mapping. *Genetics* 1994; 138(3):963-71.
- 376 20. King R, Lu L, Williams RW, Geisert EE. Transcriptome networks in the  
377 mouse retina: An exon level BXD RI database. *Mol Vis* 2015; 21:1235-51.
- 378 21. Templeton JP, Freeman NE, Nickerson JM, Jablonski MM, Rex TS,  
379 Williams RW, Geisert EE. Innate immune network in the retina activated by optic  
380 nerve crush. *Invest Ophthalmol Vis Sci* 2013; 54(4):2599-606.
- 381 22. Sun N, Shibata B, Hess JF, FitzGerald PG. An alternative means of  
382 retaining ocular structure and improving immunoreactivity for light microscopy  
383 studies. *Mol Vis* 2015; 21:428-42.
- 384 23. Takahashi H, Noda S, Imamura Y, Nagasawa A, Kubota R, Mashima Y,  
385 Kudoh J, Oguchi Y, Shimizu N. Mouse myocilin (Myoc) gene expression in ocular  
386 tissues. *Biochem Biophys Res Commun* 1998; 248(1):104-9.
- 387 24. Brubaker RF. Flow of Aqueous-Humor in Humans - the Friedenwald  
388 Lecture. *Invest Ophth Vis Sci* 1991; 32(13):3145-66.
- 389 25. Goel M, Picciani RG, Lee RK, Bhattacharya SK. Aqueous humor  
390 dynamics: a review. *Open Ophthalmol J* 2010; 4:52-9.
- 391 26. Hollows FC, Graham PA. Intra-ocular pressure, glaucoma, and glaucoma  
392 suspects in a defined population. *Br J Ophthalmol* 1966; 50(10):570-86.
- 393 27. Renard E, Palombi K, Gronfier C, Pepin JL, Noel C, Chiquet C, Romanet  
394 JP. Twenty-four hour (Nyctohemeral) rhythm of intraocular pressure and ocular  
395 perfusion pressure in normal-tension glaucoma. *Invest Ophthalmol Vis Sci* 2010;  
396 51(2):882-9.

- 397 28. Aptel F, Weinreb RN, Chiquet C, Mansouri K. 24-h monitoring devices and  
398 nyctohemeral rhythms of intraocular pressure. *Prog Retin Eye Res* 2016; 55:108-  
399 48.
- 400 29. Sommer A, Tielsch JM, Katz J, Quigley HA, Gottsch JD, Javitt J, Singh K.  
401 Relationship between intraocular pressure and primary open angle glaucoma  
402 among white and black Americans. The Baltimore Eye Survey. *Arch Ophthalmol*  
403 1991; 109(8):1090-5.
- 404 30. Cohen LP, Pasquale LR. Clinical characteristics and current treatment of  
405 glaucoma. *Cold Spring Harb Perspect Med* 2014; 4(6).
- 406 31. Gedde SJ, Panarelli JF, Banitt MR, Lee RK. Evidenced-based comparison  
407 of aqueous shunts. *Curr Opin Ophthalmol* 2013; 24(2):87-95.
- 408 32. Ojha P, Wiggs JL, Pasquale LR. The genetics of intraocular pressure.  
409 *Semin Ophthalmol* 2013; 28(5-6):301-5.
- 410 33. Ozel AB, Moroi SE, Reed DM, Nika M, Schmidt CM, Akbari S, Scott K,  
411 Rozsa F, Pawar H, Musch DC, Lichter PR, Gaasterland D, Branham K, Gilbert J,  
412 Garnai SJ, Chen W, Othman M, Heckenlively J, Swaroop A, Abecasis G,  
413 Friedman DS, Zack D, Ashley-Koch A, Ulmer M, Kang JH, Consortium N, Liu Y,  
414 Yaspan BL, Haines J, Allingham RR, Hauser MA, Pasquale L, Wiggs J, Richards  
415 JE, Li JZ. Genome-wide association study and meta-analysis of intraocular  
416 pressure. *Hum Genet* 2014; 133(1):41-57.
- 417 34. Chang TC, Congdon NG, Wojciechowski R, Munoz B, Gilbert D, Chen P,  
418 Friedman DS, West SK. Determinants and heritability of intraocular pressure and  
419 cup-to-disc ratio in a defined older population. *Ophthalmology* 2005;  
420 112(7):1186-91.
- 421 35. Carbonaro F, Andrew T, Mackey DA, Young TL, Spector TD, Hammond  
422 CJ. Repeated measures of intraocular pressure result in higher heritability and  
423 greater power in genetic linkage studies. *Invest Ophthalmol Vis Sci* 2009;  
424 50(11):5115-9.
- 425 36. van Koolwijk LM, Despriet DD, van Duijn CM, Pardo Cortes LM, Vingerling  
426 JR, Aulchenko YS, Oostra BA, Klaver CC, Lemij HG. Genetic contributions to  
427 glaucoma: heritability of intraocular pressure, retinal nerve fiber layer thickness,  
428 and optic disc morphology. *Invest Ophthalmol Vis Sci* 2007; 48(8):3669-76.
- 429 37. van Koolwijk LM, Ramdas WD, Ikram MK, Jansonius NM, Pasutto F, Hysi  
430 PG, Macgregor S, Janssen SF, Hewitt AW, Viswanathan AC, ten Brink JB,  
431 Hosseini SM, Amin N, Despriet DD, Willemse-Assink JJ, Kramer R, Rivadeneira  
432 F, Struchalin M, Aulchenko YS, Weisschuh N, Zenkel M, Mardin CY, Gramer E,  
433 Welge-Lussen U, Montgomery GW, Carbonaro F, Young TL, Group DER,  
434 Bellenguez C, McGuffin P, Foster PJ, Topouzis F, Mitchell P, Wang JJ, Wong  
435 TY, Czudowska MA, Hofman A, Uitterlinden AG, Wolfs RC, de Jong PT, Oostra  
436 BA, Paterson AD, Wellcome Trust Case Control C, Mackey DA, Bergen AA, Reis  
437 A, Hammond CJ, Vingerling JR, Lemij HG, Klaver CC, van Duijn CM. Common  
438 genetic determinants of intraocular pressure and primary open-angle glaucoma.  
439 *PLoS Genet* 2012; 8(5):e1002611.
- 440 38. Liton PB, Luna C, Challa P, Epstein DL, Gonzalez P. Genome-wide  
441 expression profile of human trabecular meshwork cultured cells,

- 442 nonglaucomatous and primary open angle glaucoma tissue. *Mol Vis* 2006;  
443 12:774-90.
- 444 39. Burdon KP, Macgregor S, Hewitt AW, Sharma S, Chidlow G, Mills RA,  
445 Danoy P, Casson R, Viswanathan AC, Liu JZ, Landers J, Henders AK, Wood J,  
446 Souzeau E, Crawford A, Leo P, Wang JJ, Rochtchina E, Nyholt DR, Martin NG,  
447 Montgomery GW, Mitchell P, Brown MA, Mackey DA, Craig JE. Genome-wide  
448 association study identifies susceptibility loci for open angle glaucoma at TMCO1  
449 and CDKN2B-AS1. *Nat Genet* 2011; 43(6):574-8.
- 450 40. Savinova OV, Sugiyama F, Martin JE, Tomarev SI, Paigen BJ, Smith RS,  
451 John SW. Intraocular pressure in genetically distinct mice: an update and strain  
452 survey. *BMC Genet* 2001; 2:12.
- 453 41. Struebing FL, Geisert EE. What Animal Models Can Tell Us About  
454 Glaucoma. *Prog Mol Biol Transl Sci* 2015; 134:365-80.
- 455 42. Sappington RM, Carlson BJ, Crish SD, Calkins DJ. The microbead  
456 occlusion model: a paradigm for induced ocular hypertension in rats and mice.  
457 *Invest Ophthalmol Vis Sci* 2010; 51(1):207-16.
- 458 43. Cone FE, Gelman SE, Son JL, Pease ME, Quigley HA. Differential  
459 susceptibility to experimental glaucoma among 3 mouse strains using bead and  
460 viscoelastic injection. *Exp Eye Res* 2010; 91(3):415-24.
- 461 44. Samsel PA, Kisiswa L, Erichsen JT, Cross SD, Morgan JE. A novel  
462 method for the induction of experimental glaucoma using magnetic  
463 microspheres. *Invest Ophthalmol Vis Sci* 2011; 52(3):1671-5.
- 464 45. Wang WH, Millar JC, Pang IH, Wax MB, Clark AF. Noninvasive  
465 measurement of rodent intraocular pressure with a rebound tonometer. *Invest*  
466 *Ophthalmol Vis Sci* 2005; 46(12):4617-21.
- 467 46. Paylakhi SH, Yazdani S, April C, Fan JB, Moazzeni H, Ronaghi M, Elahi  
468 E. Non-housekeeping genes expressed in human trabecular meshwork cell  
469 cultures. *Mol Vis* 2012; 18:241-54.
- 470 47. Ethier CR, Kamm RD, Palaszewski BA, Johnson MC, Richardson TM.  
471 Calculations of flow resistance in the juxtacanalicular meshwork. *Invest*  
472 *Ophthalmol Vis Sci* 1986; 27(12):1741-50.
- 473 48. Brubaker RF. The effect of intraocular pressure on conventional outflow  
474 resistance in the enucleated human eye. *Invest Ophthalmol* 1975; 14(4):286-92.
- 475 49. Bradley JM, Vranka J, Colvis CM, Conger DM, Alexander JP, Fisk AS,  
476 Samples JR, Acott TS. Effect of matrix metalloproteinases activity on outflow in  
477 perfused human organ culture. *Invest Ophthalmol Vis Sci* 1998; 39(13):2649-58.
- 478 50. Johnson M. 'What controls aqueous humour outflow resistance?'. *Exp Eye*  
479 *Res* 2006; 82(4):545-57.
- 480 51. Vranka JA, Kelley MJ, Acott TS, Keller KE. Extracellular matrix in the  
481 trabecular meshwork: intraocular pressure regulation and dysregulation in  
482 glaucoma. *Exp Eye Res* 2015; 133:112-25.
- 483 52. Row S, Liu Y, Alimperti S, Agarwal SK, Andreadis ST. Cadherin-11 is a  
484 novel regulator of extracellular matrix synthesis and tissue mechanics. *J Cell Sci*  
485 2016; 129(15):2950-61.
- 486

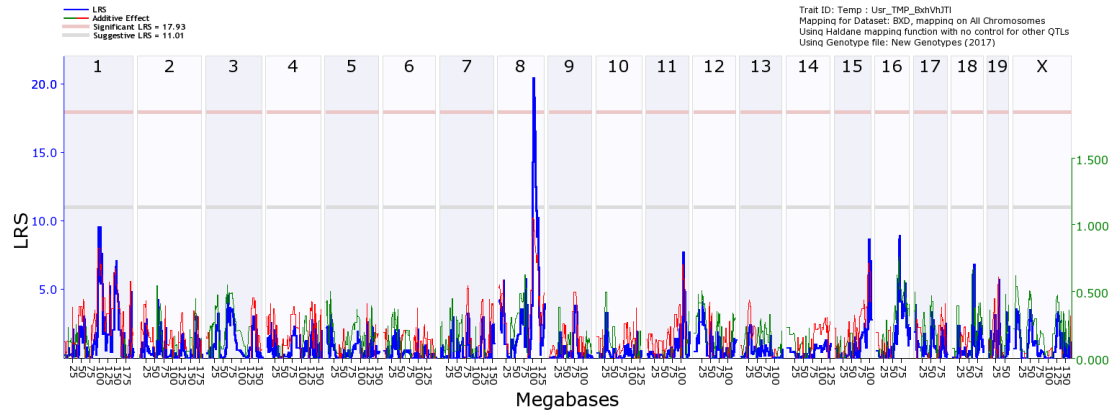
487 **Figures**  
488  
489



490  
491  
492 **Figure 1.** The distribution of IOP measurements across the BXD strains is illustrated in a  
493 bar chart with means and Standard Deviations. In the 33 strains of mice the IOP ranged  
494 from a low of 10.9 mmHg to a high of 17.1 mmHg.

495  
496  
497  
498  
499  
500  
501  
502  
503  
504  
505  
506  
507  
508

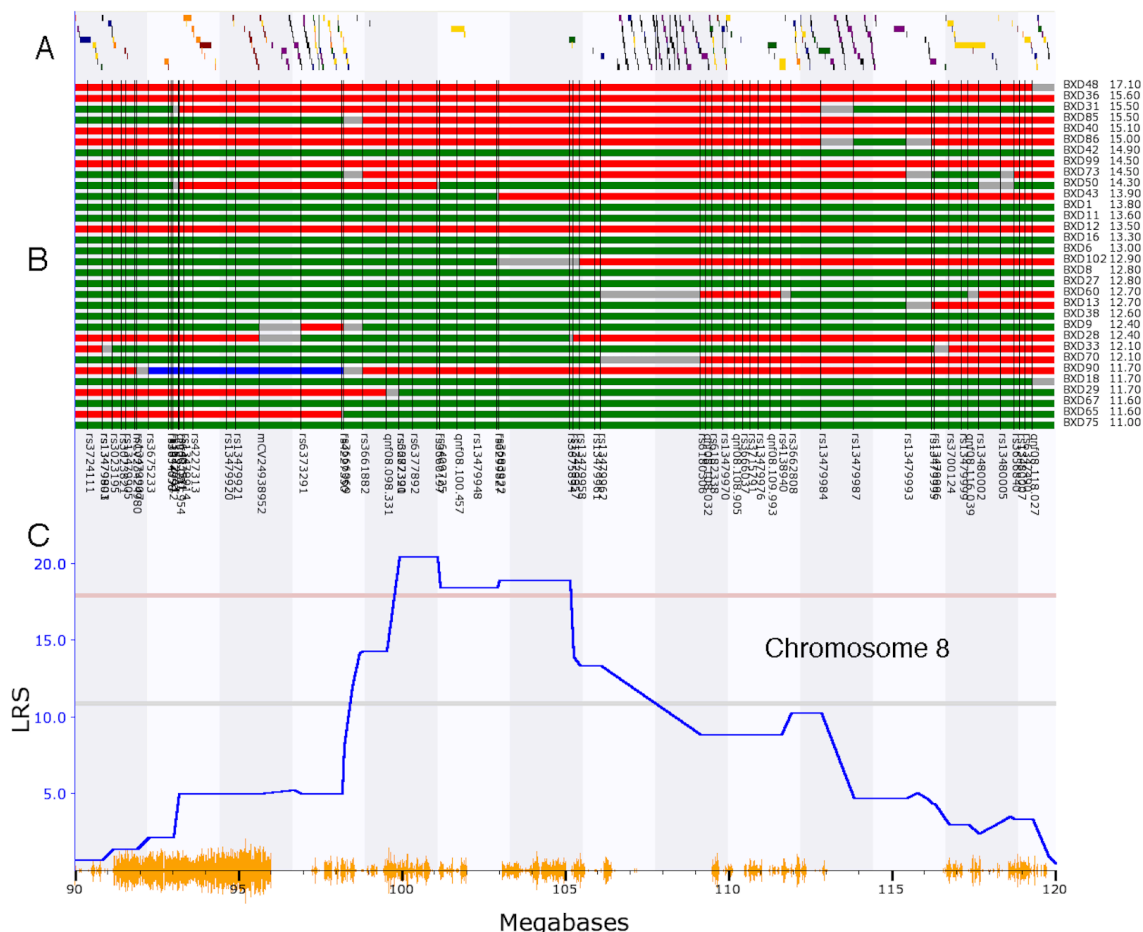




509  
510  
511  
512  
513  
514  
515  
516

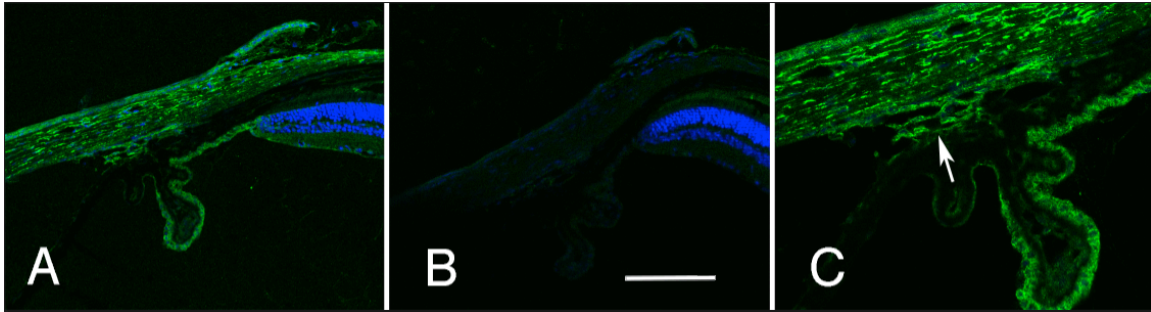
**Figure 2.** A genome-wide interval map of IOP. The interval map plots the linkage related score (LRS) across the genome from chromosome 1 to chromosome X. The light gray line is the suggestive level and the light red line is genome-wide significance ( $p = 0.05$ ). When the IOP measures were mapped to the mouse genome there was a significant association between IOP and a locus on Chromosome 8.

517  
518



519  
520 **Figure 3.** The interval map for Chr. 8: 90 to 120Mb is illustrated. A is the gene tract, that  
521 identifies the locations of known genes across the genome. B is a haplotype map for the  
522 different BXD RI strains listed to the right and ranked from the highest IOP to the lowest  
523 IOP. The location of genomic markers is indicated by black vertical lines. C is an  
524 expanded version of the interval map for IOP. Finally, the bottom trace (yellow)  
525 identified the location of SNPs between the C57BL/6 mouse and the DBA2/J mouse. The  
526 genomic location is indicated along this lower trace. Notice that the peak of the QTL in C  
527 sits in a region of the genome that contains very few known genes (A).

528  
529  
530  
531  
532



533

534

535

536

537

538

539

540

541

542

543

544

545

546

547

548

**Figure 4.** The distribution of cadherin 11 in the limbal area of the eye is illustrated. The section in A was stained with an antibody specific to cadherin 11 (green) and for DNA (blue). This staining is specific to the primary antibody for it is not observed in a section stained with the secondary antibody alone (B). The staining pattern of the trabecular meshwork is shown at higher magnification in C (arrow). A and B are taken at the same magnification and the scale bar in panel B represents 25  $\mu\text{m}$ .

**Table 1.** Primers designed for Cdh11 and Cdh8 and Myoc

<b>Cdh11</b>	Forward 5' GAAACCAAAGTCCCAGTGGCC 3'
	Reverse 5' TGGTCCATTGGCTGTGTCGT 3'
<b>Cdh8</b>	Forward 5' AGCCTCCGGTCTTCTCTTCAC 3'
	Reverse 5' CAGTGTGGCGGTCAATGGAAA 3'
<b>Myoc</b>	Forward 5' GCTGGCTACCACGGACACTT 3'
	Reverse 5' CGCTCAAGTTCCAGGTTTCGC 3'
<b>Ppia</b>	Mm_Ppia_1_SG QuantiTect Primer Assay

549